A STUDY OF IMAGE FUSION TECHNIQUES IN REMOTE SENSING

M. Hahn [a]*, F. Samadzadegan [b]

[a] Dept. of Geomatics, Computer Science and Mathematics, Stuttgart University of Applied Sciences, Stuttgart, Germany - michael.hahn@hft-stuttgart.de

[b] Dept. of Surveying and Geomatics, Faculty of Engineering, University of Tehran, Tehran, Iran - samadz@ut.ac.ir

Commission IV, WG IV/7

KEY WORDS: Image Fusion, Multi Resolution, Remote Sensing, Correlation, Quality

ABSTRACT:

The amount and variety of remote sensing imagery of varying spatial resolution is continuously increasing and techniques for merging images of different spatial and spectral resolution became widely accepted in practice. This practice, known as data fusion, is designed to enhance the spatial resolution of multispectral images by merging a relatively coarse-resolution image with a higher resolution panchromatic image taken of the same geographic area. This study examines fused images and their ability to preserve the spectral and spatial integrity of the original image. The mathematical formulation of ten data fusion techniques is worked out in this paper. Included are colour transformations, wavelet techniques, gradient and Laplacian based techniques, contrast and morphological techniques, feature selection and simple averaging procedures. Most of theses techniques employ hierarchical image decomposition for fusion.

IRS-1C and ASTER images are used for the experimental investigations. The panchromatic IRS-1C image has around 5m pixel size, the multispectral ASTER images are at a 15m resolution level. For the fusion experiments the three nadir looking ASTER bands in the visible and near infrared are chosen. The concept for evaluating the fusion methods is based on the idea to use a reduced resolution of the IRS-1C image data at 15m resolution and of the ASTER images at 45m resolution. This maintains the resolution ratio between IRS and ASTER and allows comparing the image fusion result at the 15m resolution level with the original ASTER images. This statistical comparison reveals differences between all considered fusion concepts.

INTRODUCTION

Every year the number of airborne and spaceborne data acquisition missions grows, producing more and more image data about the Earth's surface. The imagery is recorded with varying resolution and merging images of different spatial and spectral resolution has become a widely applied procedure in remote sensing. Many fusion techniques have been proposed for fusing spectral with high spatial resolution image data in order to increase the spatial resolution of the multispectral images (Carper et al., 1990; Chavez et al., 1991; Kathleen and Philip, 1994, Wald, 2002).

Data fusion as defined by Wald (2004) is a "*formal framework in which are expressed the means and tools for the alliance of data originating from different sources. It aims at obtaining information of greater quality; the exact definition of 'greater quality' will depend upon the application.* This approach is based upon the synergy offered by the various sources." Focussed to the output of airborne and spaceborne sensors, i.e. recorded images, image fusion or image data fusion is concerned with methods for the fusion of images. The emphasis in this paper is put on images taken by different sensors with different spatial resolutions. The goal is either to visualize the original sets of images with improved expressiveness regarding its inherently available information, or to produce a new product of synthesized images with a better spatial resolution. The motivation of users of image fusion techniques often comprises both aims.

Image fusion on the pixel level is sometimes also called pixel or signal fusion. If image fusion is related to the feature representation level of images it is also called feature fusion. Object or decision fusion deals with the high level representation of images by objects. The meaning of the terms feature and object in image processing (e.g. Gonzalez and Woods, 2002) and Remote Sensing (e.g. Wald, 2004) is still quite different from its use in Photogrammetry (e.g. Schenk, 2003) and Computer Vision (e.g Haralik and Shapiro, 1992). As a consequence the features in photogrammetry, in particular linear features extracted by edge detection schemes and areal features based e.g. on a texture segmentation scheme lead to an image description which is closer to an object description in image processing or pattern recognition than to a feature description. Image classification performed on a multispectral image may take in addition to the spectral data textural features and other feature image descriptions into account. At this point the difference between the different uses of terms is getting very obvious.

Data fusion in its interrelationship with image analysis and GIS was reviewed in Baltsavias and Hahn (1999). Fusion of data recorded by different sensors has been put into context to data in GIS databases. Quite long is the list of problems of fusion related problems that have been worked out in the above quoted paper. The discrepancy between scene representations given by imagery and given by corresponding maps or GIS (vector) data sets links fusion concepts to topics of image analysis with the

* Corresponding author.

consequence that feature extraction, segmentation, classification, plays a important rule in particular for decision fusion. From an application point of view this addresses problems of automating mapping procedures and map update.

In the following we will focus in image fusion techniques on the pixel level. The most well-known techniques, the IHS and PCA methods for colour composing, are already implemented in remote sensing packages; but some more advanced methods are methodologically or technically not yet mature. Altogether ten techniques will be mathematically described in the next section. All algorithms are implemented in MATLAB with the idea to create a MATLAB fusion toolbox. Experiments with IRS-1C and ASTER images are presented and discussed in Section 4. We finally conclude with a short summary and recommendations for future research.

2. IMAGE FUSION TECHNIQUES

The number of proposed concepts for image fusion is growing which indicates ongoing research in this area. Technically, image data recorded by different sensors have to be merged or composed to generate a new representation. Alternatively data from one sensor are also subject of image fusion. Different multispectral channels are to be considered as different sources, as well as images taken at different times by the same sensor.

The goal of all image fusion techniques is obtain information of greater quality which may consist of a more accurate description of the scene than any of the individual source images. This fused image should be more useful for human visual inspection or machine perception. The sensors used for image fusion need to be accurately co-aligned. Alternatively images from different sources may have to be registered or geocoded to the reference coordinate system.

References for the algorithms worked out in the following are Anderson (1987); Burt (1992); Carper et al. (1990); Chavez et al. (1991); Kathleen and Philip (1994), Rockinger (1996) and Wald (2002). With respect to the conceptual approach, we distinguish the proposed techniques into eight classes of IHS, PCA, SWDT, Laplacian and FSD Pyramid, Contrast pyramid, Gradient pyramid, Selection and simple Averaging process. The main characteristics of these techniques are discussed in the context of its mathematical formulation.

1.1 Fusion based on Intensity-Hue-Saturation (IHS) method

The Intensity-Hue-Saturation method (IHS) is one of the most popular fusion methods used in remote sensing. In this method, three multispectral bands *R*, *G* and *B* of low resolution are first transformed to the IHS colour space:

$$\begin{bmatrix} I \\ V_1 \\ V_2 \end{bmatrix} = \begin{bmatrix} \frac{1}{3} & \frac{1}{3} & \frac{1}{3} \\ \frac{1}{\sqrt{6}} & \frac{1}{\sqrt{6}} & -\frac{2}{\sqrt{6}} \\ \frac{1}{\sqrt{2}} & -\frac{1}{\sqrt{2}} & 0 \end{bmatrix} \begin{bmatrix} R \\ G \\ B \end{bmatrix}, \quad (1)$$

$$H = \tan^{-1}\left(\frac{V_2}{V_1}\right), \quad (2)$$

$$S = \sqrt{V_1^2 + V_2^2} \quad (3)$$

Here I is intensity, H is hue, S is saturation, and V_1, V_2 are intermediate variables. Fusion proceeds by replacing I with the panchromatic high-resolution image of another source. The fused image is then obtained by performing an inverse transformation from IHS back to the original RGB space according to

$$\begin{bmatrix} R \\ G \\ B \end{bmatrix} = \begin{bmatrix} 1 & \frac{1}{\sqrt{6}} & \frac{1}{\sqrt{2}} \\ 1 & \frac{1}{\sqrt{6}} & -\frac{1}{2} \\ 1 & -\frac{2}{\sqrt{6}} & 0 \end{bmatrix} \begin{bmatrix} I \\ V_1 \\ V_2 \end{bmatrix} \quad (4)$$

For some more discussion of this standard technique please confer to Carper et al. (1990).

2.2. Fusion based on Principal Component Analysis method

Principal component analysis (PCA) is a general statistical technique that transforms multivariate data with correlated variables into one with uncorrelated variables. These new variables are obtained as linear combination of the original variables. PCA has been widely used in image encoding, image data compression, image enhancement and in image fusion. Applied to image fusion, PCA is performed on the image with all its spectral bands. An orthogonal colour coordinate system for PCA is derived by

$$\begin{bmatrix} PC1 \\ PC2 \\ PC3 \end{bmatrix} = \begin{bmatrix} \Phi_{11} & \Phi_{12} & \Phi_{13} \\ \Phi_{21} & \Phi_{22} & \Phi_{23} \\ \Phi_{31} & \Phi_{32} & \Phi_{33} \end{bmatrix} \begin{bmatrix} R \\ G \\ B \end{bmatrix} \quad (5)$$

$$H = \tan^{-1}\left(\frac{PC3}{PC2}\right) \quad , \quad S = \sqrt{PC2^2 + PC3^2} \quad (6)$$

Hue (H) and saturation (S) defined here are different to values obtained by IHS (Eq. 2). The transformation matrix Φ with elements Φ_{ij} consist of the eigenvectors of the covariance matrix R with terms r_{ij} and the transformation matrix satisfies the relationship

$$\Phi R \Phi^T = \Lambda \quad (7)$$

where $\Lambda = diag(\Lambda_1, \Lambda_2, \Lambda_3)$ are eigenvalues corresponding to Φ organised in descend order. The procedure to merge the RGB and the Pan image using the PCA method is similar to the IHS method. That is, the first component (PC1) of the PCA space is replaced by the Pan image and retransformed back into the original RGB space:

$$\begin{bmatrix} R_{new} \\ G_{new} \\ B_{new} \end{bmatrix} = \begin{bmatrix} \Phi_{11} & \Phi_{12} & \Phi_{13} \\ \Phi_{21} & \Phi_{22} & \Phi_{23} \\ \Phi_{31} & \Phi_{32} & \Phi_{33} \end{bmatrix}^T \begin{bmatrix} pan \\ PC2 \\ PC3 \end{bmatrix} \quad (8)$$

2.3 Fusion method based on a shift invariant extension of the DWT

More recently, the wavelet transform has been used for merging data derived from different resolution sensors (Rockinger, 1996). To overcome the shift dependency of the wavelet fusion method, the input images must be decomposed into a shift invariant wavelet representation. For convenience, we summarize this approach for the case of 1D input signals.

As for the discrete wavelet transform (DWT), each stage of the shift invariant DWT (SIDWT) splits the input sequence into the wavelet sequence $W_i(n)$ and the scale sequence $S_i(n)$ which serves as input for the next decomposition level (Rockinger, 1996):

$$W_i(n) = \sum_k g(2^i.k).s_i(n-k) \tag{9}$$

$$s_{i+1}(n) = \sum_k h(2^i.k).s_i(n-k) \tag{10}$$

The zero'th level scale sequence is set equal to the input sequence $S_0(n) = f(n)$, thus defining the complete SIDWT decomposition scheme. In contrast to the standard DWT decomposition scheme the subsampling is dropped, resulting in a highly redundant wavelet representation. The analysis filters $g(2^i.k)$ and $h(2^i.k)$ at level i are obtained by inserting the appropriate number of zeros between the filter taps of the prototype filters $g(k)$ and $h(k)$.

The reconstruction of the input sequence is performed by the inverse SIDWT as a convolution of both shift invariant wavelet sequence and scale sequence with the appropriate reconstruction filters $\tilde{g}(2^i.k)$ and $\tilde{h}(2^i.k)$ as follows:

$$s_i(n) = \sum_k \tilde{h}(2^i.n-k).s_{i+1}(n) + \sum_k \tilde{g}(2^i.n-k).w_{i+1}(n) \tag{11}$$

2.4. Fusion based on a Laplacian pyramid method

The Laplacian filtered image can be realized as a difference Gaussian filtered images. Accordingly the Laplacian pyramid is obtainable from the Gaussian pyramid. Let G^k be the k^{th} $(k = 1,...,N)$ level of the Gaussian pyramid for an image *I*. Then

$$\begin{cases} G^0 = I \\ G^{K+1} = \left[w * G^K\right]_{\downarrow 2} \quad \text{for} \quad \text{k} = 1,..., \text{N} - 1 \end{cases} \tag{13}$$

where the kernel w is obtained a discrete Gaussian density, '*' denotes two-dimensional convolution and the notation $[...]_{\downarrow 2}$ indicates that the image in brackets is down-sampled by 2 (in both, horizontal and vertical directions) which is accomplished by selecting every other point in the filtered image. The Gaussian pyramid is a set of lowpass filtered copies of the image, each with a cut-off frequency one octave lower than its predecessor. The Laplacian pyramid is determined by

$$\begin{cases} L^N = G^N \\ L^k = G^k - 4\omega * \left[G^{k+1}\right]_{\uparrow 2} \quad \text{for} \quad \text{k} = 0,..., \text{N} - 1 \end{cases} \tag{14}$$

where the notation $[...]_{\uparrow 2}$ indicates that the image inside the brackets is up-sampled by 2 (in both the horizontal and vertical directions). Here, convolution by the Gaussian kernel has the effect of interpolation by a low-pass filter.

The Laplacian pyramid transform decomposes the image into multiple levels. Each level in the Laplacian pyramid represents the result of convolving the original image with a difference of two Gaussian functions thus each successive level is a band-passed, sub-sampled and scaled version of the original image.

The Laplacian pyramid has a perfect reconstruction property; the original image can be reconstructed by reversing the Laplacian pyramid operations:

$$\begin{cases} \hat{G}^N = L^N \\ \hat{G}^k = L^k + 4\omega * \left[\hat{G}^{k+1}\right]_{\uparrow 2} \quad \text{for} \quad \text{k} = 0,..., \text{N} - 1 \end{cases} \tag{15}$$

$\hat{G}^0$ is identical to the original image *I*.

Fusion is performed in the Laplacian pyramid domain by constructing a fused pyramid. The pyramid coefficient (or hyperpixel) at each location in the fused pyramid is obtained by selecting the hyperpixel of the sensor pyramid that has the largest absolute value. Let L_A and L_B be the Laplacian pyramids of two images *A* and *B*. With L_F the fused pyramid is denoted which is determined by

$$L_F^K(i,j) = \begin{cases} L_A^K(i,j) & \text{if} \quad \left|L_A^K(i,j)\right| > \left|L_B^K(i,j)\right| \\ L_B^K(i,j) & \text{Otherwise} \end{cases} \tag{16}$$

where *k* is the level of the pyramid and (*i,j*) denotes a hyperpixel at that level (Sharma, 1999).

2.5. Fusion method based on Contrast pyramids

Toet (1990) introduced an image fusion technique which preserves local luminance contrast in the sensor images. The technique is based on selection of image features with maximum contrast rather than maximum magnitude (Sharma, 1999). It is motivated by the fact that the human visual system is based on contrast and hence the resulting fused image will provide better details to a human observer. The pyramid decomposition used for this technique is related to luminance processing in the early stages of the human visual system which are sensitive to local luminance contrast (Toet, 1990). Fusion is performed using the multiresolution contrast pyramid. The k^{th} level R_k of the contrast pyramid is obtained by:

$$\begin{cases} R_k = \dfrac{G_k}{4w * \left[G_{k+1}\right]_{\uparrow 2}} \quad \text{for} \quad \text{k} = 1,..., \text{N} - 1 \\ R_N = G_N \end{cases} \tag{17}$$

The hyperpixels of the contrast pyramid *R* are related to the local luminance contrast. Luminance contrast *C* is defined as:

$$C = \frac{L - L_b}{L_b} = \frac{L}{L_b} - 1 \tag{18}$$

where L is the luminance at a certain location in the image and L_b is the luminance of the local background. The denominator

in the equation for R_k represents the up-sampled and interpolated version of G_{k+1}. A hyperpixel in this interpolated image corresponds to a weighted local average in the neighbourhood of the hyperpixel at the same location in G_k. Hence, the denominator in R_k is proportional to L_b whereas the numerator is proportional to L. Therefore the pyramid whose levels are $R_k - I_k$ (where I_k is the k^{th} level of the unit pyramid with all hyperpixels having value 1) represents a contrast pyramid. The original image can be perfectly reconstructed by reversing the pyramid generation operations described above.

The fused contrast pyramid R_F is formed from the contrast pyramids R_A and R_B of the images A and B by using the selection rule:

$$R_F^k(i,j) = \begin{cases} R_A^k(i,j) & \text{if } \left|R_A^k(i,j)\right| > \left|R_B^k(i,j)\right| \\ R_B^k(i,j) & \text{Otherwise} \end{cases} \quad (19)$$

where k is the level of the pyramid and (i, j) denote the hyperpixels at that level. The fusion rule selects the hyperpixels corresponding to the largest local luminance contrast. As a result, image features with high contrast are preserved in the fused image.

2.6. Fusion method based on FSD Laplacian pyramids

The filter-subtract-decimate (FSD) hierarchical pyramid proposed by Anderson (1987) is conceptually identical with the the Laplacian concept explained in section 2.4.

In the following we refer to the input image as G_0 the low-pass filtered versions are G_1 to G_N with decreasing resolutions and the corresponding difference images are L_0 to L_N, respectively. A recursive procedure for the creation of the FSD pyramid reads as follows:

$$\begin{aligned} G_{n+1}^0 &= W * G_n \\ L_n &= G_n - G_{n+1}^0 \\ G_{n+1} &= \text{Subsampled } G_{n+1}^0 \end{aligned} \quad (20)$$

With the Gaussian filter *W* the process for fusion coincides with the Laplacian concept outlined above (Section 2.4).

2.7. Fusion method based on Gradient pyramids

Fusion based on gradient pyramids is another alternative to the Laplacian concept. As above a first step consist of constructing a Gaussian pyramid. Burt and Kolczynski (1993) used the *5 x 5* Gaussian kernel

$$w = \dot{w} * \dot{w} \quad (21)$$

to lowpass filter the image with

$$\dot{w} = \frac{1}{16}\begin{bmatrix} 1 & 2 & 1 \\ 2 & 4 & 2 \\ 1 & 2 & 1 \end{bmatrix} \quad (22)$$

Down-sampling by a factor of two in horizontal and vertical directions recursive processing over successive levels produces a Gaussian pyramid.

The next step in image decomposition is extracting the orientation gradient details on each level (except the top) of the Gaussian pyramid. Burt calls this step creating the orientation gradient pyramid (Burt and Kolczynski, 1993). It is called the orientation gradient because the kernels are the gradient filters d_1 through d_4 :

$$D_{kl} = d_l * \left[G_k + \dot{w} * G_k\right] \quad (23)$$

$$d_1 = \begin{bmatrix} 1 & -1 \end{bmatrix},\ d_2 = \begin{bmatrix} 0 & -1 \\ 1 & 0 \end{bmatrix},\ d_3 = \begin{bmatrix} -1 \\ 1 \end{bmatrix},\ d_4 = \begin{bmatrix} -1 & 0 \\ 0 & 1 \end{bmatrix} \quad (24)$$

D_{kl} are the details for level *k* and orientation *l*, G_k is the level *k* input from the reduced image pyramid. The process for fusion follows the concept outlined in Section 2.4.

2.8. Fusion method based on Morphological pyramids

Mathematical morphology offers another conceptual approach to image fusion. The morphological filters, in particular opening and closing are employed for creating a morphological pyramid (Morales et al., 1995). The filters are designed to preserve edges or shapes of objects, while eliminating noise and details in an image. The morphological opening followed by-closing and closing followed by opening are chosen because they are biased-reduced operators. The morphological pyramid is constructed by successively morphological filtering and down-sampling:

$$I_L = [(I_{(L-1)} \circ K) \bullet K]_{\downarrow d} \qquad L = 0,1,...,n \quad (25)$$

where L is the pyramid level. I_0 is the original image, $[\ldots]_{\downarrow d}$ represents down sampling by a factor of *d* in both spatial dimension, $(I \circ K)$ represents the morphological opening of the image *I* with structuring element *K*, and $(I \bullet K)$ represents the morphological closing. The finest level L=0 of the morphological pyramid contains the input image. The image at any level *L* is created by applying morphological filtering with a 3x3 structuring element to the image level *(L-1)* followed by down-sampling the filtered image with *d=2*. The process for fusion follows the concept outlined in Section 2.4.

2.9. Fusion method based on Averaging

A simple approach for fusion, based on the assumption of additive Gaussian noise, consists of synthesizing the fused image by averaging corresponding pixels of the sensor images**.** Averaging should work well (Sharma, 1999) when the images to be fused are from the same type of sensor and contain additive noise only. If the variance of noise in *q* sensor images is equal then averaging them reduces the variance of noise in the fused image according to the error propagation law.

2.10. Fusion method based on Selection

Fusion based on some selection process is an alternative to simple averaging. Selection may use the Laplacian pyramid as basis. This technique has then three distinct stages - pyramid construction, selection of pyramid coefficients based on a

salience metric, and construction of the fused image from the fused pyramid coefficients. The salience metric is e.g the energy (or squared sum) of pyramid coefficients in an area of e.g. 5×5 hyper-pixels. Minimum and maximum criteria are used for the selection. The last step is to apply the inverse transform to obtain the fused image (Sharma, 1999).

3. MATLAB IMPLEMENTATION

All described algorithms have been implemented in MATLAB. Behind this MATLAB development is the idea to design and implement a toolbox for image fusion. This toolbox can be easily extended to other fusion proposals and – and this is probably the more important issue – it can be combined with a variety of other MATLAB functions like image registration and sensor orientation. At the time of writing this paper quality measures and metrics to assess and compare the quality of image fusion products (e.g the Image Noise Index method, Leung et.al. 2001) could not be implemented to a sufficient extent. Ideas are published and intensively discussed on this issue e.g. by the ERSel Special Interest Group (Wald, 2004).

Figure 1. Matlab user interface of image rectification and fusion

Figure 1 gives an impression of one of the graphical user interfaces (GUI) of the toolbox. Of course, all developed MATLAB functions can be applied without GUI too.

4. EXPERIMENTS AND RESULTS

The above described algorithms are applied to fuse IRS-1C and ASTER images. The panchromatic IRS-1C has 5m pixel size; the multispectral ASTER images have 15m pixels. The ASTER bands B_1, B_2, B_3 are used in the experiments. Both images are shown in Figure 2. Due to scaling of the pictures the difference in resolution of both images is not visible in Figure 2.

The concept for evaluating the fusion methods is based on the idea to use a reduced resolution of the IRS-1C image data at 15m resolution and of the ASTER images at 45m resolution. This maintains the resolution ratio between IRS and ASTER and allows comparing the image fusion result at the 15m resolution level with the original ASTER images as well as the IRS image at 5 m resolution. Correlation is used for statistical comparison of the fusion result with the original images.

Figure 2. Panchromatic IRS-1C image (left), and ASTER original bands of B_1, B_2, B_3 in RGB format

The application of the data fusion algorithms leads to 10 different fused images. The result of the wavelet fusion method is shown as one example in Figure 3. All other fused images are not plotted due to the lack of space.

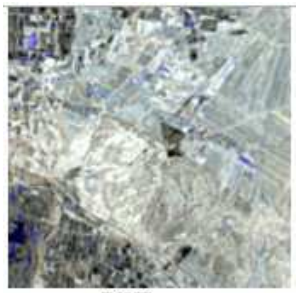

Figure 3. Fusion result for the ASTER bands

The difference can be already noticed visually. To get a first statistical quantification normalized cross-correlation is computed between the different fusion results and the original intensity (table and graphic in Figure 4) and spectral image channels (table and graphic in Figure 5) which serve as a kind of ground truth.
Correlation values with around 60% in the worst case and around 90% in the best case can be noticed in these figures. Altogether a quite homogenous appearance over all 12 results can be noticed. (Note: the DWT and the shift invariant DWT and the selection with min and max criteria have been introduced separately in the table). Correlation differences of plus or minus 5 % in the correlation values are already visually noticeable. Nevertheless the limited significance of the correlation value for the expressiveness of the fusion result demands for more sophisticated quality measures.

5. CONCLUSION

The goal of this paper to study fusion techniques has been approached by formulation a great variety of different fusion procedures. The mathematical formulation of ten data fusion techniques is worked out which includes colour transformations, wavelet techniques, gradient and Laplacian based techniques, contrast and morphological techniques, feature selection and simple averaging procedures.

Quality related investigations based on correlation showed a fairly homogenous appearance in terms of the correlation values over all fusion results. A detailed look at the fusion result reveals differences between the different procedures, which have to be investigated further with more sophisticated quality measures. Regarding the quality issues the paper delivers an intermediate report of an ongoing research.

Method	Correlation		
	B1	B2	B3
Average	0.74	0.74	0.75
Contrast	0.76	0.77	0.76
DWT	0.82	0.82	0.82
FSD	0.84	0.84	0.85
Gradient	0.84	0.84	0.85
Laplacian	0.82	0.82	0.82
Morphological	0.78	0.78	0.77
PCA	0.87	0.86	0.89
IHS	0.86	0.81	0.83
SIDWT	0.83	0.82	0.83
Select Max	0.80	0.87	0.90
Select Min	0.62	0.67	0.65

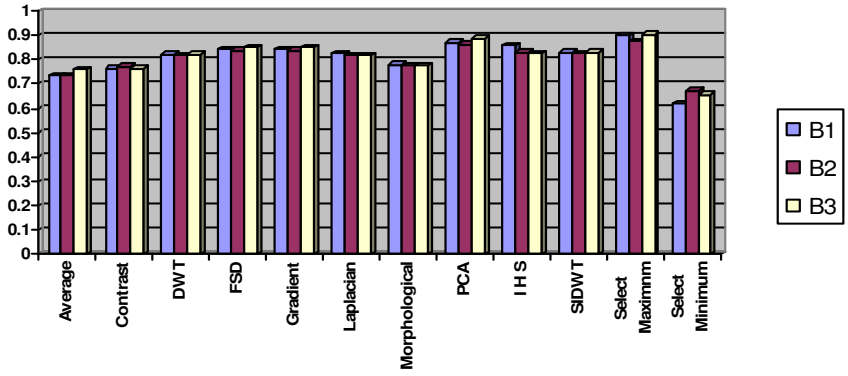

Figure 4.The intensity correlation of the output of different fusion techniques with the original panchromatic IRS-1C band.

Method	Correlation		
	B1	B2	B3
Average	0.71	0.72	0.73
Contrast	0.76	0.76	0.74
DWT	0.72	0.72	0.73
FSD	0.73	0.73	0.74
Gradient	0.73	0.74	0.75
Laplacian	0.72	0.73	0.74
Morphological	0.71	0.71	0.69
PCA	0.71	0.73	0.73
IHS	0.72	0.73	0.71
SIDWT	0.73	0.74	0.75
Select Max	0.56	0.60	0.64
Select Min	0.82	0.79	0.78

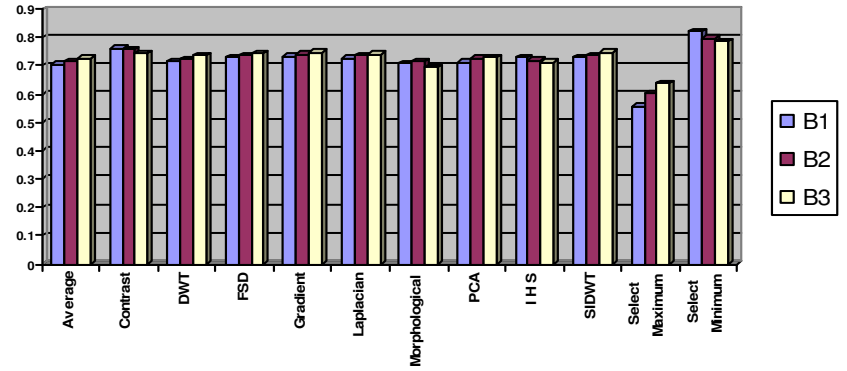

Figure 5.The spectral correlation of the output of different fusion techniques with the B_1, B_2, B_3 of original ASTER bands.

REFERENCES

Anderson, C.H., 1987. A Filter-Subtract-Decimate Hierarchical Pyramid Signal Analyzing and Synthesizing Technique, United States Patent 4,718,104, Washington, D.C.

Baltsavias, E., Hahn, M., 1999: Integration of Image Analysis and GIS. In: International Archives of Photogrammetry and Remote Sensing, Vol. 32, Part 7-4-3W6, pp. 12 - 19, Joint ISPRS/EARSeL Workshop, Valladolid, 3-4 June 1999

Burt , P.J., Kolczynski,, R. J., 1993. Enhanced image capture through fusion, In Fourth International Conference on Computer Vision, pages 173-182. IEEE Computer Society.

Carper, W.J., Lilesand, T.W., Kiefer, R.W., 1990. The use of Intensity-Hue-Saturation transformation for merging SPOT panchromatic and multispectral image data, PE&RS 56 (4) 459–467.

Chavez , P.S., Sides, S.C., Anderson, J.A., 1991. Comparison of three different methods to merge multiresolution and multispectral data: Landsat TM and SPOT panchromatic, PE&RS (57) 295-303.

Gonzalez, R.C., Woods, R.E., 2002. Digital Image Processing, 2nd Edition, Prentice Hall.

Haralik, R.M., Shapiro, L.G., 1992. Computer and Robot vision, Vol. 1, Addison-Wesley Publishing Company, Reading, MA.

Kathleen, E., Philip, A.D., 1994. The use of intensity-hue-saturation transform for producing color shaded relief images, PE&RS. (60) 1369-1374.

Leung, L.W., King, B., Vahora, V., 2001. Comparison of image data fusion techniques using Entropy and INI. Asian Conf. of Remote Sensing, Singapore.

Morales, A., Acharya, T., Ko, S., 1995. Morphological pyramids with alternating sequential filters, IEEE Trans. Image Processing, vol.4, pp. 965-977.

Rockinger, O., 1996. Image Sequence Fusion Using a Shift-Invariant Wavelet Transform, Systems Technology Research, Intelligent Systems Group Daimler Benz AG Alt Moabit 96 A, 10559 Berlin, Germany.

Schenk, T., 2003. From Data to Information and Knowledge. Joint ISPRS Workshop "Challenges in Geospatial Analysis, Integration and Visualization II", Stuttgart.

Sharma, R.K., 1999. Probabilistic Model-based Multisensor Image Fusion, Oregon Graduate Institute of Science and Technology, PH.D Thesis.

Toet, A., 1990. Hierarchical image fusion. Machine Vision and Applications, 3:1-11.

Wald, L., 2002. Data Fusion: Definitions and Architectures - Fusion of Images of Different Spatial Resolutions, Les Presses de l'Ecole des Mines, Paris, France.

Wald, L., 2004. The data fusion server.
http://www.data-fusion.org/(accessed 28. April 2004).